

# UC Irvine

## Faculty Publications

### Title

Regional budgets for nitrogen oxides from continental sources: Variations of rates for oxidation and deposition with season and distance from source regions

### Permalink

<https://escholarship.org/uc/item/39q997bg>

### Journal

Journal of Geophysical Research, 103(D7)

### ISSN

0148-0227

### Authors

Munger, J. William  
Fan, Song-Miao  
Bakwin, Peter S.  
[et al.](#)

### Publication Date

1998-04-01

### DOI

10.1029/98JD00168

### License

<https://creativecommons.org/licenses/by/3.0/> 4.0

Peer reviewed

## Regional budgets for nitrogen oxides from continental sources: Variations of rates for oxidation and deposition with season and distance from source regions

J. William Munger, Song-Miao Fan,<sup>1</sup> Peter S. Bakwin,<sup>2</sup> Mike L. Goulden,<sup>3</sup> Allen. H. Goldstein,<sup>4</sup> Albert S. Colman,<sup>5</sup> and Steven C. Wofsy

Division of Engineering and Applied Sciences and Department of Earth and Planetary Sciences, Harvard University, Cambridge, Massachusetts

**Abstract.** Measurements of nitrogen deposition and concentrations of NO, NO<sub>2</sub>, NO<sub>y</sub> (total oxidized N), and O<sub>3</sub> have been made at Harvard Forest in central Massachusetts since 1990 to define the atmospheric budget for reactive N near a major source region. Total (wet plus dry) reactive N deposition for the period 1990–1996 averaged 47 mmol m<sup>-2</sup> yr<sup>-1</sup> (126 μmol m<sup>-2</sup> d<sup>-1</sup>, 6.4 kg N ha<sup>-1</sup> yr<sup>-1</sup>), with 34% contributed by dry deposition. Atmospheric input adds about 12% to the N made available annually by mineralization in the forest soil. The corresponding deposition rate at a distant site, Schefferville, Quebec, was 20 mmol m<sup>-2</sup> d<sup>-1</sup> during summer 1990. Both heterogeneous and homogeneous reactions efficiently convert NO<sub>x</sub> to HNO<sub>3</sub> in the boundary layer. HNO<sub>3</sub> is subsequently removed rapidly by either dry deposition or precipitation. The characteristic (*e*-folding) time for NO<sub>x</sub> oxidation ranges from 0.30 days in summer, when OH radical is abundant, to ~1.5 days in the winter, when heterogeneous reactions are dominant and O<sub>3</sub> concentrations are lowest. The characteristic time for removal of NO<sub>x</sub> oxidation products (defined as NO<sub>y</sub> minus NO<sub>x</sub>) from the boundary layer by wet and dry deposition is ~1 day, except in winter when it decreases to 0.6 day. Biogenic hydrocarbons contribute to N deposition through formation of organic nitrates but are also precursors of reservoir species, such as peroxyacetylnitrate, that may be exported from the region. A simple model assuming pseudo first-order rates for oxidation of NO<sub>x</sub>, followed by deposition, predicts that 45% of NO<sub>x</sub> in the northeastern U.S. boundary layer is removed in 1 day during summer and 27% is removed in winter. It takes 3.5 and 5 days for 95% removal in summer and winter, respectively.

### 1. Introduction

Human activities have greatly increased the inputs of nitrogen oxides to the atmosphere (we define nitrogen oxides as follows: NO<sub>x</sub> = NO + NO<sub>2</sub>, radicals that rapidly interconvert, within minutes to hours; and NO<sub>y</sub> = NO<sub>x</sub> + NO<sub>3</sub> + N<sub>2</sub>O<sub>5</sub> + HNO<sub>3</sub> + peroxyacetylnitrate (PAN) + other organic nitrates + aerosol nitrate, the family of radicals and nonradicals that interconvert and are deposited on longer timescales *i.e.*, hours to days) [Davidson, 1991; Galloway *et al.*, 1995; Logan, 1983; Prather *et al.*, 1995]. Anthropogenic emissions of NO<sub>x</sub> (mainly from combustion) exceed the natural inputs of fixed

nitrogen to the atmosphere in North America and other urbanized regions. Photochemical production of O<sub>3</sub> in the troposphere is controlled by NO<sub>x</sub> radicals. Deposition of NO<sub>y</sub> (along with NH<sub>3</sub>) contributes to nutrient loading and acidification in sensitive ecosystems. Remote regions with low inputs from natural NO<sub>x</sub> sources may be especially sensitive to even small increases in reactive N because chemical and ecological effects are nonlinear functions of concentration [Liu *et al.*, 1987; Wedin and Tilman, 1996]. The lifetime for NO<sub>y</sub> removal determines the distance from the source region over which N levels are perturbed from the natural background. Holland *et al.* [1997] note that uncertainties in predicted global distribution of nitrogen deposition lead to large differences in estimates of global carbon uptake associated with N fertilization.

Dentener and Crutzen [1993] noted the absence of a strong seasonality in wet deposition of NO<sub>3</sub><sup>-</sup> over Europe and North America and argued that rates for production and removal of HNO<sub>3</sub> from the boundary layer are similar throughout the year, with increased rates of HNO<sub>3</sub> formation by heterogeneous hydrolysis of N<sub>2</sub>O<sub>5</sub> in winter compensating for reduced rates of homogeneous oxidation of NO<sub>2</sub> by OH. However, the contribution from dry deposition was not included, and seasonal trends in wet deposition alone may be misleading. Total annual nitrate deposition fluxes have been estimated at sites in North America by inferring the dry deposition from aver-

<sup>1</sup> Now at Atmospheric and Oceanic Sciences Program, Princeton University, Princeton, New Jersey.

<sup>2</sup> Now at Climate Monitoring and Diagnostics Laboratory, National Oceanic and Atmospheric Administration, Boulder, Colorado.

<sup>3</sup> Now at Department of Earth System Science, University of California, Irvine.

<sup>4</sup> Now at Department of Environmental Science, Policy, and Management, University of California, Berkeley.

<sup>5</sup> Now at Department of Geology and Geophysics, Yale University, New Haven Connecticut.

Copyright 1998 by the American Geophysical Union.

Paper number 98JD00168.  
0148-0227/98/98JD-00168\$09.00

age concentrations [Hanson and Lindberg, 1991; Johnson and Lindberg, 1992; Meyers et al., 1991], but long-term records of NO<sub>x</sub> and NO<sub>y</sub> concentrations and total (wet plus dry) nitrogen deposition fluxes have not been available to define seasonal cycles in the reactive nitrogen budget.

In 1990 we began continuous measurements of concentrations and eddy-covariance fluxes of NO<sub>y</sub>, concentrations of NO<sub>x</sub> and O<sub>3</sub>, and deposition of NO<sub>3</sub><sup>-</sup> in precipitation at Harvard Forest in central Massachusetts. Additional measurements were made during the Arctic Boundary Layer Expedition (ABLE 3B) experiment in the summer of 1990 near Schefferville, Quebec. Munger et al. [1996] (hereinafter referred to as M96) demonstrated that NO<sub>y</sub> eddy fluxes can be reliably determined for extended periods by eddy-covariance measurements, identified horizontal and vertical transport and chemical reaction as dominant processes controlling dry deposition of NO<sub>y</sub> to the forest canopy, and noted the absence of stomatal influence on NO<sub>y</sub> dry deposition. In this paper we examine the seasonal trends in total nitrogen deposition, evaluate the mean lifetimes for oxidation of NO<sub>2</sub> and deposition of NO<sub>y</sub> in the boundary layer, and estimate the rate of nitrogen removal during transport from source regions for the period 1990 through 1996.

## 2. Site Description and Measurement Methods

Harvard Forest is located in Petersham, Massachusetts (42.53°N, 72.18°W), at an elevation of 340 m. Within 100 km the surroundings are largely rural with a mix of mostly small (population of ~10<sup>4</sup>) and a few medium (population of ~10<sup>5</sup>) towns surrounded by forests. Extensive urban areas with relatively high NO<sub>x</sub> emission densities lie within 200-500 km to the southwest of Harvard Forest (Figure 1). Average NO<sub>x</sub> emissions given in the National Acid Precipitation Assessment Program (NAPAP) inventory within 250 km of Harvard Forest are 214 μmol m<sup>-2</sup> d<sup>-1</sup> [Environmental Protection Agency (EPA), 1989], ranging from 417 μmol m<sup>-2</sup> d<sup>-1</sup> in the southwest quadrant, which includes the New York metro-

politan area, to 75 μmol m<sup>-2</sup> d<sup>-1</sup> in the mostly rural northwest quadrant. The Boston metropolitan area is 100 km to the east; however, the prevailing winds are westerly, and emissions from Boston rarely reach the site. Harvard Forest is similar in many respects to much of the northeastern United States outside the urban corridor along the coast.

The ABLE 3B tower site was located 13 km NW of Schefferville, Quebec, Canada (54.83°N, 66.67°W), at an elevation of 500 m. Observations were made from mid-June to mid-August 1990. Besides Schefferville (largely abandoned and being demolished) and a few small villages the nearest habitations were >200 kilometers away. Schefferville is hundreds of km from major NO<sub>x</sub> sources, except when forest fires are burning nearby; it represents a remote receptor site several days' transport time from major sources of NO<sub>x</sub>, in contrast to Harvard Forest, which is immediately adjacent to a major source region.

Concentrations of NO were measured by using O<sub>3</sub> chemiluminescence. Concentrations of NO<sub>2</sub> and NO<sub>y</sub>, respectively, were measured by using Xe-lamp photolysis and catalysis by hot Au with H<sub>2</sub>, to convert NO<sub>2</sub> and NO<sub>y</sub> to NO. Dry-deposition fluxes of NO<sub>y</sub> were determined by eddy covariance. Concentrations of O<sub>3</sub> at eight heights in the forest were determined by UV absorbance. Concentrations and fluxes of O<sub>3</sub> above the canopy were determined by using a fast-response C<sub>2</sub>H<sub>4</sub>-chemiluminescent analyzer. Full details of the measurements are given by M96.

At both sites, precipitation was collected above the canopy in a polyethylene funnel that opened only during precipitation events. The sample drained to a fractionating collector housed in a refrigerator. Concentrations of NO<sub>3</sub><sup>-</sup>, SO<sub>4</sub><sup>2-</sup>, and Cl<sup>-</sup> were determined by ion chromatography. The analytical precision for rainwater analyses, determined from replicate analysis of samples and standards, was 2% or better. Additional data on precipitation composition at the National Atmospheric Deposition Program (NADP) Quabbin Reservoir site (42.392°N, 72.345°W) were obtained from the NADP data archive (<http://nadp.nrel.colostate.edu/NADP/>, National Atmospheric

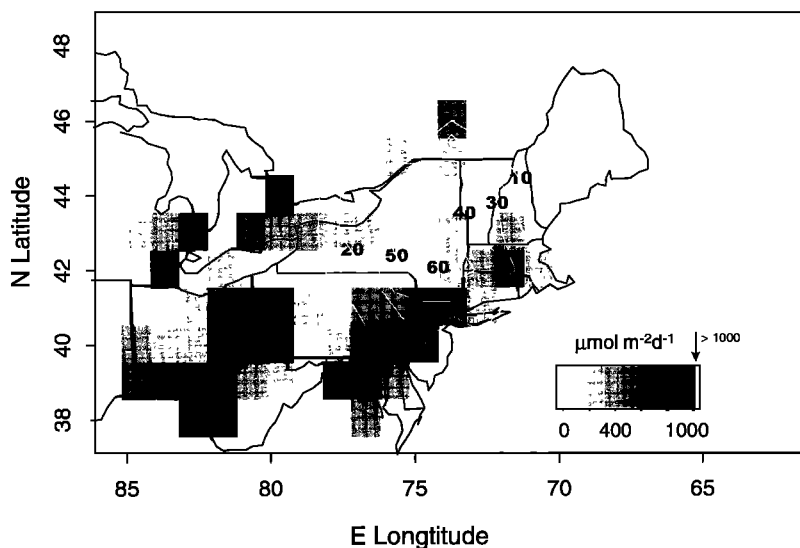


**Figure 1.** Location of Harvard Forest, indicated by cross, in relation to NO<sub>x</sub> emission densities (NAPAP emission inventory [EPA, 1989]) in the northeastern United States. Darker colors indicate increasing emission density. The origin points of 8-hour back trajectories [Moody et al., 1998] are indicated by contours showing the number of trajectories (of a total of 1276) originating in a cell.

Deposition Program (NRSP-3)/National Trends Network, August, 1997, NADP/NTN Coord. Off., Ill. State Wat. Surv., Champaign, Ill., hereinafter referred to as NADP, 1997). Wet-deposition fluxes at Harvard Forest were corrected for missed samples or inefficient collection by multiplying the amount of precipitation recorded at a standard gauge located about 1 km from the tower (R. Lent, unpublished Harvard Forest data archives, 1997) by the volume-weighted average concentration for the event (for undersampled events) or by the monthly volume-weighted average (for missed events). Fresh and recently fallen snow-core samples were collected above polyethylene sheets set out at several locations within  $\approx 50$  m radius prior to a snow event. At Schefferville, rain volumes collected by the fractionating collector were used to compute rainfall amounts because rainfall in the area was topographically influenced [Fitzjarrald and Moore, 1994] and the nearest standard rain gauge was some distance away. Collection efficiency for light misting rains accompanied by winds may be less than 100% for the precipitation funnel. When rain was reported at the site, but sample was partially lost (spill or depth for the rain gauge network [Fitzjarrald and Moore, 1994] was used.

### 3. Results

#### 3.1. Sampling Statistics

Inevitably, long-term data sets are incomplete, and the simple sum of all the data does not provide total flux over the sampling interval. Gaps occur as a result of routine instrument calibrations, periodic shutdowns, sensor malfunctions, and other problems (e.g., lightning strikes, and power fail-

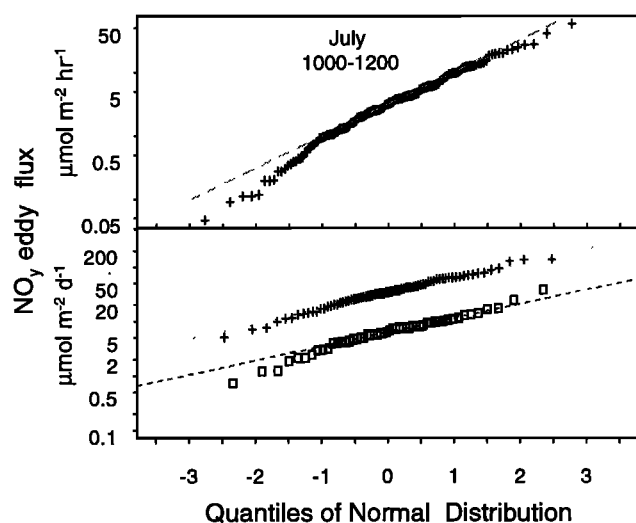


**Figure 2.** (top) Distribution of hourly NO<sub>y</sub> eddy flux values for observations made between 1000 and 1200 during days in July. Data are plotted against quantiles of a normal distribution. A lognormally distributed data set would plot on a straight line. The dashed line connects the upper and lower quartiles of the data. (bottom) Daily integrated NO<sub>y</sub> eddy fluxes for July at Harvard Forest (pluses) and for the ABL 3B Schefferville site (squares). The dotted line connects the tenth and ninetyth percentile of the Harvard Forest data; the dashed line connects twenty-fifth and seventy-fifth percentile of the Schefferville data.

ures). Individual observations may not be truly independent. Diel variations, synoptic patterns, and seasonal trends introduce autocorrelation into the data. For example, the lagged correlation of mean midday NO<sub>y</sub> eddy fluxes is 0.25 for a 1 day lag and exceeds 0.1 for lags up to 40 days. These correlations must be properly accounted for in filling data gaps and aggregating the data to monthly, seasonal, and annual timescales [Goulden *et al.*, 1996a].

Hourly observations of NO<sub>y</sub> eddy flux consist of a central population that fits a lognormal distribution with some low outliers, as illustrated by the July data from Harvard Forest (Figure 2, top). Other time periods show similar patterns but with different ranges and median values. Integrated daily fluxes at Harvard Forest for each month (illustrated for July) and for Schefferville also fit a lognormal distribution over the central portion of their range (Figure 2, bottom). NO<sub>y</sub> eddy fluxes had a mean diel cycle with a morning maximum (M96); the period 1000 to 1200 contributed nearly 20% of the integrated daily eddy flux. We have aggregated the data in monthly increments, consistent with observed autocorrelation, to provide a sufficient number of observations from each hour of the day to obtain accurate means and still resolve seasonal variations. Means are computed independently for each hour of the day, and the mean diel cycle is summed to give mean daily flux for each month. The median or geometric mean represents the central tendency of lognormally distributed data. However, we use the arithmetic mean here because it incorporates important contributions from infrequent high-deposition events that may provide a significant fraction of total deposition during an averaging interval.

Half the NO<sub>y</sub> eddy flux input at Schefferville, and during the summers at Harvard Forest, was deposited in extreme events on 25% and 20% of the days, respectively. Increasing skewness and contribution from rare events leads to greater potential for sampling error from missed data. We therefore examined the uncertainty associated with missing data by generating random subsamples of the data. The means (or medians) of subsamples containing  $\geq 50\%$  of the data vary by 10–15%. Variability increases sharply as more data are excluded (Figure 3). We estimated the uncertainty of the NO<sub>y</sub> eddy-flux totals by computing the standard deviation of random subsamples that include 50% of the data from each interval.

On account of the smaller sample size for Schefferville data, individual days were integrated separately. Missing data were interpolated between adjacent points; days with fewer than 20 hours of valid data were rejected, and daily totals were computed. These values were used to obtain a seasonal mean, and estimates of the sampling uncertainty were derived from the standard deviation of data from valid days.

#### 3.2. Combined Deposition

**3.2.1. Harvard Forest.** Monthly average concentrations of NO<sub>3</sub><sup>-</sup> in rainwater at Harvard Forest (Figure 4, top) compared closely with the long-term means for rain sampled at the nearby NADP Quabbin reservoir site, implying that precipitation collected at Harvard Forest is regionally representative. The annual volume-weighted mean concentration of NO<sub>3</sub><sup>-</sup> at Harvard Forest was 25  $\mu\text{mol l}^{-1}$ , with a minimum of  $\sim 20$   $\mu\text{mol l}^{-1}$  in fall and winter and a maximum of 30  $\mu\text{mol l}^{-1}$  in early summer. Daily inputs of NO<sub>3</sub><sup>-</sup> by precipitation ranged from  $< 1$   $\mu\text{mol m}^{-2} \text{d}^{-1}$  for a trace of rain to  $> 2000$   $\mu\text{mol m}^{-2} \text{d}^{-1}$

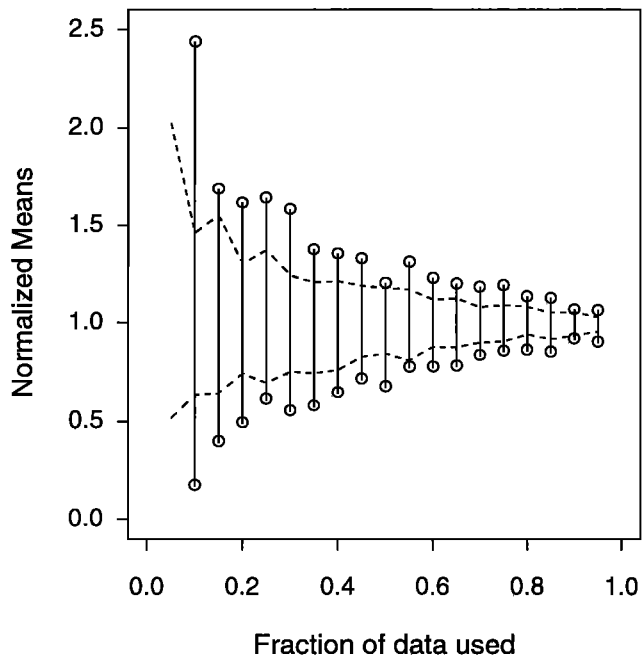


**Figure 3.** Mean values computed for 100 random subsamples drawn from the set of all  $\text{NO}_y$  eddy-flux data for the period 1000-1200 in July and August. The ranges of these means are normalized by the overall mean and plotted against the fraction of data used in the subsamples. The dashed lines show the corresponding range of mean values for subsamples drawn from a random lognormal distribution based on the mean and standard deviation of the original data.

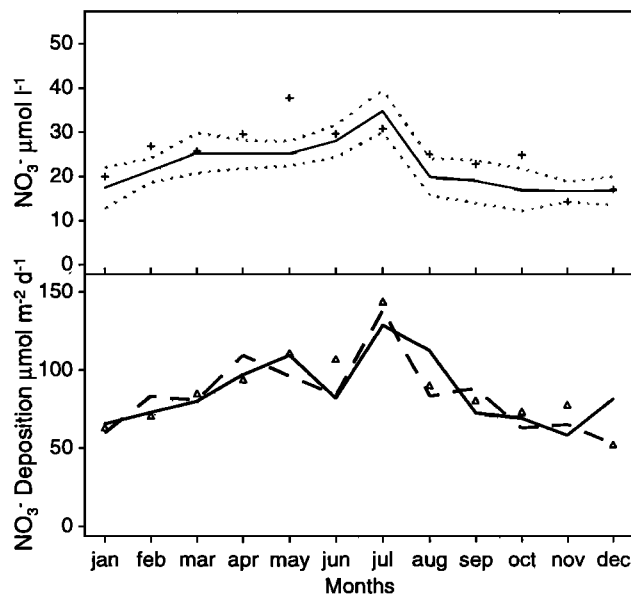


**Figure 4.** (top) Average  $\text{NO}_3^-$  concentrations in rainwater at Harvard Forest (pluses) and at the Quabbin Reservoir National Atmospheric Deposition site (NADP, 1997) for the period 1982 through June 1996 (solid line); dashed lines are the standard error of the monthly means for the Quabbin data. (bottom) Mean  $\text{NO}_3^-$  deposition by precipitation at Harvard Forest for the period 1990-1995 (solid line) and at the Quabbin Reservoir NADP site (dashed line). The overall mean for the period 1982-1996 at the Quabbin site is given by open triangles.

for a particularly dirty ( $\text{NO}_3^- = 100 \mu\text{mol l}^{-1}$ ) large event. The distribution of wet-deposition data at Harvard Forest was highly skewed; 13% of the events with largest inputs contributed half the wet deposition of  $\text{NO}_3^-$ , a more significant influence of extreme events than that for dry deposition. Wet deposition of  $\text{NO}_3^-$  (Figure 4, bottom) peaked in summer at Harvard Forest, as observed at Quabbin Reservoir and other NADP sites in the northeastern United States (NADP, 1997).

Daily integrated  $\text{NO}_y$  eddy fluxes measured by eddy covariance ranged from near 0 to  $470 \mu\text{mol m}^{-2} \text{d}^{-1}$ . Mean daily dry-deposition fluxes of  $\text{NO}_y$  at Harvard Forest for monthly intervals generally showed low values in winter and higher values in summer or fall (Figure 5). The integrated daily  $\text{NO}_y$  eddy fluxes show seasonal differences that were not observed in the midday mean eddy fluxes because of day length differences and the strong diel cycle in  $\text{NO}_y$  eddy fluxes during summer months (M96). Monthly deposition (wet plus dry) of reactive N for the 7 years beginning January 1, 1990 (Figure 6) exhibited values of around  $200 \mu\text{mol m}^{-2} \text{d}^{-1}$  during the growing seasons of all years except 1995, which had an exceptional drought. Eddy fluxes (dry deposition) of N during the summer of 1990 were higher, and nitrate wet deposition was lower than that in subsequent years. Unusual meteorological conditions may be responsible, but possible artifacts from a change in the  $\text{NO}_y$  catalyst (M96) cannot be ruled out. Nevertheless, conclusions drawn from the 7-year data set are not significantly different from the 6-year data set excluding 1990. Variations in wet inputs tended to compensate for changes in dry deposition. The decline in dry deposition during 1994 (Figure 5) was offset by increased wet deposition, and the total deposition (Figure 6) was comparable to previous years. However, reduced wet deposition during a severe drought in summer 1995 was not offset by increased

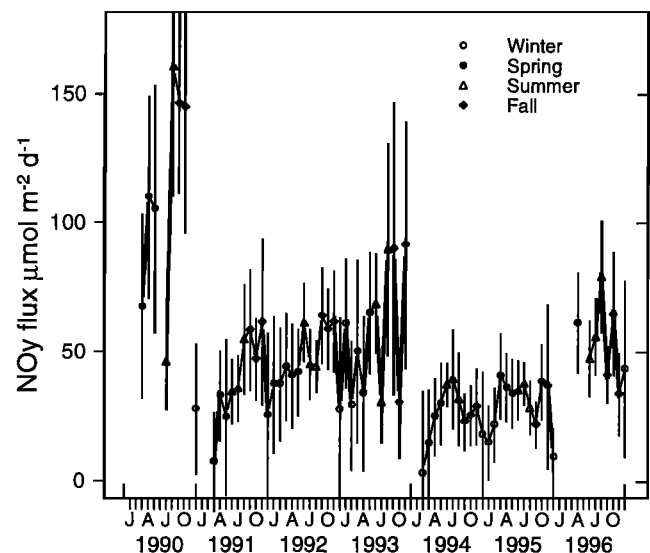


**Figure 5.** Mean  $\text{NO}_y$  dry-deposition fluxes computed for monthly time intervals. Mean fluxes are computed for 50 random subsamples separately for each hour of the day and then summed to give the mean value of integrated daily  $\text{NO}_y$  dry-deposition flux during that month. Vertical segments give the standard deviation of the 50 subsample means. The seasons, winter (DJF), spring (MAM), summer (JJA), and fall (SON) are denoted by different symbols as indicated in the legend.

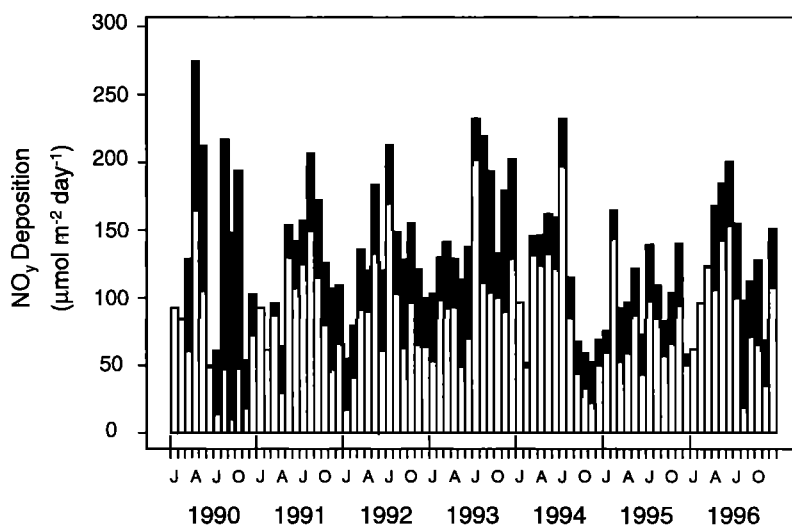


**Figure 6.** Total (wet plus dry) monthly NO<sub>y</sub> deposition at Harvard Forest for the period 1990-1996. Light shading indicates the monthly precipitation input; dark shading is the dry deposition (see Figure 5).

dry deposition. Total NO<sub>y</sub> inputs on an annual basis, averaged  $47 \pm 7.4$  (sum of monthly means plus or minus monthly standard deviation)  $\text{mmol m}^{-2} \text{yr}^{-1}$  (Figure 7) with 34% contributed by dry deposition. Total reactive N deposition was highest in summer and early fall ( $4\text{--}5 \text{ mmol m}^{-2} \text{month}^{-1}$ ;  $150 \mu\text{mol m}^{-2} \text{d}^{-1}$ ) and decreased by about a factor of 2 in winter months. Peak deposition rates coincide with highest fraction of NO<sub>x</sub> oxidation products (minima in NO<sub>x</sub>:NO<sub>y</sub>) and not with the maximum NO<sub>y</sub> concentrations, which are highest in winter (M96).

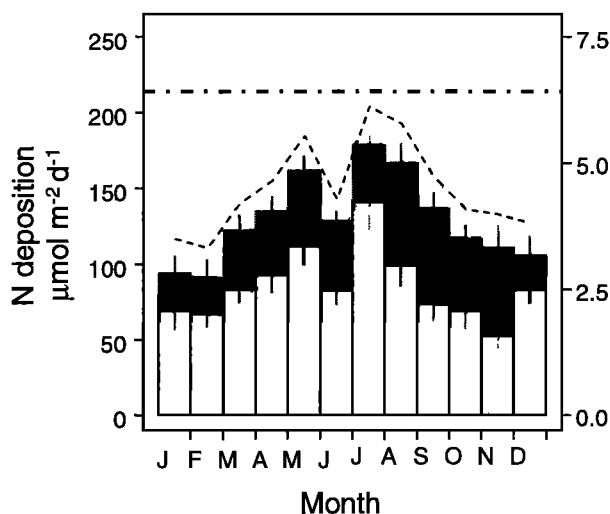


**Figure 7.** Monthly mean deposition of reactive N at Harvard Forest computed from the 1990-1996 data. Dark shading (upper bar) is the input from dry deposition, light shading (lower bar) is the precipitation input. The thin vertical lines indicate the sampling uncertainty for each monthly estimate determined from the standard deviation of the means of random subsamples of the data. The dashed lines are the overall sampling uncertainty for the total deposition. The dot-dashed line indicates the mean NO<sub>x</sub> emission rate within 250 km radius of Harvard Forest given by NAPAP emission inventories [EPA, 1989].

**3.2.2. Schefferville.** The overall volume-weighted NO<sub>3</sub><sup>-</sup> concentration in rainwater at the Schefferville tower site was  $3.8 \mu\text{mol l}^{-1}$ , roughly a factor of 10 less than that at Harvard Forest in summer. Nitrate deposition in rainwater varied from  $0.4 \mu\text{mol m}^{-2} \text{d}^{-1}$  to  $120 \mu\text{mol m}^{-2} \text{d}^{-1}$ , with a mean and median of 15 and  $7 \mu\text{mol m}^{-2} \text{d}^{-1}$ , respectively. Seven days (14%) of a total of 50 rainy days accounted for 50% of the NO<sub>3</sub><sup>-</sup> wet deposition, indicating that sporadic advection of pollutants was very important. A single event with  $\sim 10 \mu\text{mol l}^{-1}$  [NO<sub>3</sub><sup>-</sup>] on July 30, which has been identified as an anthropogenic pollution event [Bakwin *et al.*, 1994], contributed 17% of the wet deposition during the period.

Integrated daily NO<sub>y</sub> eddy fluxes were  $0.7\text{--}37 \mu\text{mol m}^{-2} \text{d}^{-1}$  (M96, Figure 5), with a mean and median of 7.6 and  $6.4 \mu\text{mol m}^{-2} \text{d}^{-1}$ , respectively. Dry-deposition fluxes of nitrate were more uniform than wet-deposition fluxes; daily totals exceeded  $14 \mu\text{mol m}^{-2} \text{d}^{-1}$  on only 4 days (Figure 8). Total NO<sub>y</sub> inputs ranged from  $<5$  to  $130 \mu\text{mol m}^{-2} \text{d}^{-1}$ , with a mean value of  $18.5 \mu\text{mol m}^{-2} \text{d}^{-1}$  ( $0.55 \text{ mmol m}^{-2} \text{month}^{-1}$ ), about 12% of the deposition rate at Harvard Forest during summer. Dry deposition contributed 41% of the total reactive N deposition at the Schefferville site, compared to 77% during the same period at Harvard Forest. On average, however, dry deposition contributed 35% of the total reactive N deposited during summer at Harvard Forest.

### 3.3. Regional Comparisons

Deposition rates for N determined at 20 northeastern U.S. sites in the National Dry Deposition Network (NDDN) and the Integrated Forest Study (IFS) ranged from 24 to  $68 \text{ mmol m}^{-2} \text{yr}^{-1}$  (mean 43) [Johnson and Lindberg, 1992; Meyers *et al.*, 1991]. The deposition rates determined in these studies by inferential method are consistent with the eddy-covariance measurements at Harvard Forest. Estimated contributions from dry deposition at IFS and NDDN sites fell in the range 30-70%, which is comparable to results of direct measurements from Harvard Forest and Schefferville. Nitrogen deposition fluxes at Harvard Forest were intermediate between deposition at West Point, New York ( $56 \text{ mmol m}^{-2} \text{yr}^{-1}$ ) and Howland, Maine ( $34 \text{ mmol m}^{-2} \text{yr}^{-1}$ ), consistent with the

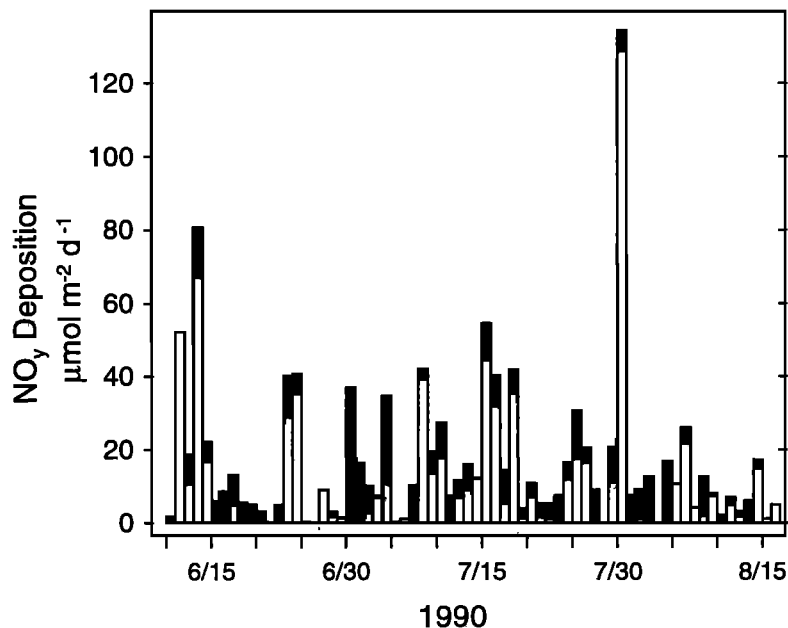


**Figure 8.** Total reactive N deposition at Schefferville during summer 1990. Precipitation inputs are shown as light shading; dry deposition is shown as dark shaded bar. Days with too many missing data are seen as gaps in the dry-deposition time series.

southwest-to-northeast decline in N deposition across the region noted by *Ollinger et al.* [1993]. No clear seasonal cycle in total N deposition was apparent across the NDDN [*Meyers et al.*, 1991], although the West Point site in New York had a summer maximum during 2 of 3 years studied. The seasonal trends at Harvard Forest become most apparent when many years of data are aggregated; this finding illustrates the value of long-term data sets in identifying underlying patterns that may be masked by atmospheric variability (e.g. wet summer in 1991 and dry summer in 1990).

### 3.4. Ammonium Inputs

Reduced nitrogen in the form of NH<sub>3</sub> and NH<sub>4</sub><sup>+</sup> in precipitation and dry deposition also contributes biologically available N. We did not measure NH<sub>4</sub><sup>+</sup> in precipitation at Harvard Forest, but we can estimate it from the measured SO<sub>4</sub><sup>2-</sup> inputs at Harvard Forest and mean NH<sub>4</sub><sup>+</sup>:SO<sub>4</sub><sup>2-</sup> ratio in precipitation collected at the Quabbin Reservoir NADP site (NADP, 1997) (Figure 9). Estimated wet deposition of NH<sub>4</sub><sup>+</sup> (8.1 mmol m<sup>-2</sup> yr<sup>-1</sup>) was ≈15% of the total NO<sub>3</sub><sup>-</sup> input at Harvard Forest. *Tjepkema et al.* [1981] observed low concentrations and deposition of NH<sub>3</sub> at Harvard Forest and estimated that aerosol deposition of NH<sub>4</sub><sup>+</sup> added 4.3 mmol m<sup>-2</sup> yr<sup>-1</sup>. Recent measurements [*Lefer*, 1997] (B.L. Lefer et al., Nitric acid and ammonia at a rural northeastern U.S. site, submitted to *Journal of Geophysical Research*, 1997) confirm that NH<sub>3</sub> levels are low at Harvard Forest.

## 4. Discussion

### 4.1. Atmospheric Contribution to Ecosystem Nitrogen Pools

Atmospheric N deposition at Harvard Forest is significant in comparison with the N turnover by vegetation but small in relation to the total N content of vegetation and soils. Total N

in the near-surface soil (5410 mmol m<sup>-2</sup>) at a nearby hardwood stand [*Aber et al.*, 1993] represents about 90 years accumulation at present rates for nitrate plus ammonium deposition (60.4 mmol N m<sup>-2</sup> yr<sup>-1</sup>). Combined input of atmospheric nitrate and ammonium also appears small (~12%) in comparison with the annual net N mineralization rate of 500 mmol m<sup>-2</sup> yr<sup>-1</sup> [*Aber et al.*, 1993]. If atmospheric inputs of N are distributed uniformly within these pools, deposition may have only small effects on the ecosystem, although long-term cumulative effects might be important [*Wedin and Tilman*, 1996]. However, atmospheric inputs of N are roughly half the green foliar N content (100-150 mmol m<sup>-2</sup>) and nearly equal to the N deposited in litter (60-70 mmol m<sup>-2</sup> yr<sup>-1</sup>). Foliar absorption of N could lead to more significant effects by

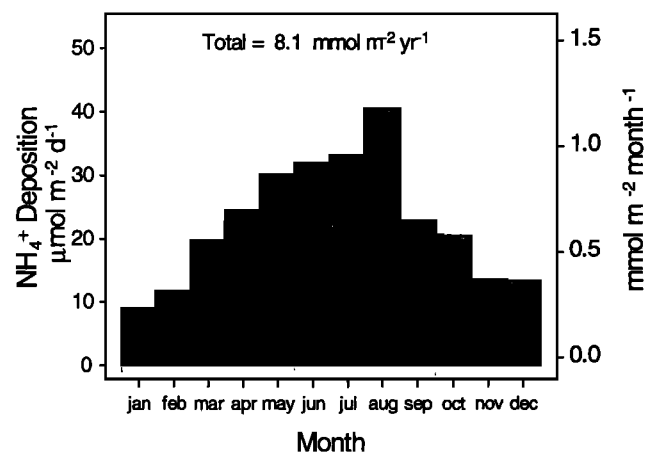


**Figure 9.** Estimated NH<sub>4</sub>-N input from precipitation at Harvard Forest determined from the NH<sub>4</sub><sup>+</sup>:SO<sub>4</sub><sup>2-</sup> ratio at Quabbin Reservoir NADP site (NADP, 1997) and the measured SO<sub>4</sub><sup>2-</sup> deposition in precipitation at Harvard Forest.

**Table 1.** Quarterly Statistics for N deposition and Meteorological Conditions at Harvard Forest

Season <sup>a</sup>	Year	Total N Deposition, μmol m <sup>-2</sup> d <sup>-1</sup>	Frequency of Surface Winds by Sector			Frequency of Rain <sup>b</sup> , %	Rainfall amount <sup>b</sup> , mm
			Northwest (270°- 45°), %	East (45°-180°), %	Southwest (180°-270°), %		
Spring	1990	205	46.6	12.8	40.2	50.0	337.9
Summer	1990	139	40.3	21.9	37.2	39.1	271.3
Fall	1990	132	44.7	16.8	38.0	30.8	263.8
Winter	1991	103	52.9	15.3	31.4	40.1	311.2
Spring	1991	105	57.1	17.0	25.7	35.8	309.6
Summer	1991	168	51.1	17.5	31.0	33.8	420.0
Fall	1991	135	48.3	16.3	35.2	35.2	408.4
Winter	1992	81	55.6	16.0	28.1	39.4	210.6
Spring	1992	146	47.2	26.9	25.9	34.8	293.9
Summer	1992	161	48.0	16.6	35.1	49.8	390.5
Fall	1992	135	46.5	19.1	34.2	46.2	272.1
Winter	1993	110	48.8	24.4	26.5	47.6	222.8
Spring	1993	128	45.1	26.7	28.0	53.4	282.1
Summer	1993	197	51.5	15.3	32.9	53.3	356.0
Fall	1993	168	34.5	20.1	44.8	60.4	357.6
Winter	1994	116	49.2	21.0	29.5	47.6	357.6
Spring	1994	151	44.2	19.2	36.1	53.3	362.1
Summer	1994	169	32.6	18.5	48.4	47.9	474.5
Fall	1994	59	54.8	19.0	25.6	28.0	NA
Winter	1995	103	52.4	20.5	26.7	28.9	370.0
Spring	1995	103	49.0	23.9	26.9	33.7	262.6
Summer	1995	107	38.3	19.5	41.3	29.4	200.1 <sup>c</sup>
Fall	1995	108	42.3	24.0	33.5	34.1	472.4
Winter	1996	58	52.1	21.5	26.1	38.6	252.7
Spring	1996	159	46.2	18.9	34.8	31.5	322.9
Summer	1996	151	40.2	18.0	41.5	26.7	NA
Fall	1996	103	50.9	21.6	27.1	NA	NA

<sup>a</sup> We define the seasons as follows; winter is December through February, spring is March through May, summer is June through August, and fall is September through November

<sup>b</sup> NA signifies periods with gaps in the precipitation data record.

<sup>c</sup> Invalid rain gauge data for June-August 1995 have been replaced by data from an adjacent site about 10 km north.

atmospheric N, and atmospheric input of N, if it is efficiently converted to woody biomass, with C:N ratio = 200, could support carbon storage rate of 1.6 t C ha<sup>-1</sup> yr<sup>-1</sup> [Schindler and Bayley, 1993], comparable to the net carbon accumulation observed at Harvard Forest for the period 1991-1995 (1.4-1.8 ton-C ha<sup>-1</sup> yr<sup>-1</sup>) [Goulden *et al.*, 1996b].

#### 4.2. Meteorological and Seasonal Factors

Nitrogen deposition measured at Harvard Forest depends on wind patterns that control transport from source regions, frequency and amount of precipitation, oxidizing capacity of the atmosphere, and other factors. Mean NO<sub>y</sub> concentrations and eddy fluxes were higher for periods with southwesterly winds, the direction associated with transport from east coast urban areas, and with trajectories originating in the Great Lakes/Ohio Valley region [Moody *et al.*, 1998] (see Table 1). Periods with frequent wet weather or above average rainfall amounts are also associated with enhanced N deposition. A least-squares fit to a linear model of the data that predicts N deposition by season, the percentage of winds from the SW sector, and the frequency of rainfall gave a multiple R<sup>2</sup> of 0.65 (see Table 2a). The regression model identifies a significant (p < 0.01) seasonal component with an amplitude of 40 μmol m<sup>-2</sup> d<sup>-1</sup> (Table 2b) accounting for 38% of the variance in the data. The variations in N deposition due to differences in frequency of SW wind and precipitation account for an additional 17% and 11% of variance, respectively. Each of

the estimated effects for the observed range of SW wind and precipitation frequency is about 30 μmol m<sup>-2</sup> d<sup>-1</sup>. We attribute the influence of wind direction to advection from source regions and the influence of precipitation frequency on scavenging processes. We argue below that the seasonal dependence of NO<sub>y</sub> deposition is due to differences in chemical processing.

#### 4.3. Influence of Rates for Oxidation of NO<sub>2</sub> on NO<sub>y</sub> Deposition Flux

**4.3.1. Estimated HNO<sub>3</sub> production rates.** As M96 noted, direct deposition of NO<sub>2</sub> is a small contribution to the dry deposition of NO<sub>y</sub>; HNO<sub>3</sub> and organic nitrates (see below) account for NO<sub>y</sub> dry deposition. Aerosol nitrate and HNO<sub>3</sub> are the sources of nitrate in precipitation. In this section we evaluate the seasonal pattern of production rates for depositing species, HNO<sub>3</sub> and organic nitrates that can be derived from the observed concentrations at Harvard Forest, and compare it with the observed deposition rates. We will consider two inorganic pathways for production of HNO<sub>3</sub>: homogeneous oxidation of NO<sub>x</sub>,



and heterogeneous oxidation, via reactions (2)-(4), culminating in hydrolysis of N<sub>2</sub>O<sub>5</sub> on aerosol surfaces. Photolysis, reaction (5), terminates this pathway.

**Table 2a.** Regression Results for the Linear Model fit of N Deposition Predicted by Seasonality and Frequency of Precipitation

Analysis of Variance Results				
Predictor	Degrees of Freedom	Sum of Squares	Mean Square	Pr(F) <sup>a</sup>
Season	3	12,930	4,311.0	0.002
SW winds	1	5,930	5,930.0	0.006
Frequency of precipitation	1	3,597	3,597.0	0.026
Residual	19	11,700	615.7	

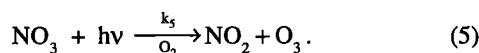
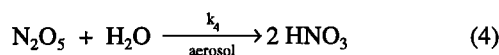
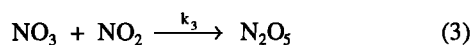
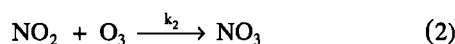
  

Regression coefficients <sup>b</sup>		
Factor	Coefficient	Standard Error
Intercept (a <sub>0</sub> ), μmol m <sup>-2</sup> d <sup>-1</sup>	129	5.0
season 1, μmol m <sup>-2</sup> d <sup>-1</sup>	-8	9.2
season 2, μmol m <sup>-2</sup> d <sup>-1</sup>	16	8.6
season 3, μmol m <sup>-2</sup> d <sup>-1</sup>	16	10.0
SW winds, μmol m <sup>-2</sup> d <sup>-1</sup> % <sup>-1</sup>	2.0	1.1
Frequency of Precipitation, μmol m <sup>-2</sup> d <sup>-1</sup> % <sup>-1</sup>	1.5	0.6

$$N_{\text{DEP}} = a_0 + \sum a_1 s_j + a_2 \text{SW} + a_3 \text{FP} + \epsilon.$$

<sup>a</sup> Probability based on F distribution for the given degrees of freedom that the observed trends are random.

<sup>b</sup> Regression coefficients are computed for the intercept (annual mean), the seasonal factors, which are transformed to obtain ordered orthogonal factors [Chambers and Hastie, 1992], and the response to changes in percentage of time with SW wind and to changes in frequency of rain.



We also consider one organic pathway based on formation of hydroxyalkyl nitrates from biogenic hydrocarbons. Oxidation of alkenes by OH generates peroxy radicals that react with NO to form hydroxyalkyl nitrates. The reported yield of hydroxyalkyl nitrates from isoprene reaction is 12% [Paulson and Seinfeld, 1992; Tuazon and Atkinson, 1990], though it could be less than 5% (Chen *et al.*, submitted to *Journal of Geophysical Research*, 1997). A yield of 17% has been observed for  $\alpha$ -pinene [Noziere *et al.*, 1997]. Shorter (2-4 carbon) hydroxyalkyl nitrates have significant Henry's Law constants [Kames and Schurath, 1992; Roberts, 1990; Shepson *et al.*, 1996] and will dissolve in precipitation or on aerosol. The unsaturated hydroxyalkyl nitrates from isoprene may have similar solubility and, in addition, react with OH [Shepson *et al.*, 1996]. Expected products include dinitrates, acid nitrates, and acetyl nitrate, which readily hydrolyzes [Trainer *et al.*, 1991]. Aerosol nitrate has been observed in smog-chamber reactions of biogenic hydrocarbons [Hoffmann *et al.*, 1997].

Although the detailed chemistry of hydroxyalkyl nitrates has not been worked out, atmospheric models that include them assume they have a deposition velocity and rainfall scavenging efficiency equal to that of HNO<sub>3</sub> [Horowitz *et al.*, 1998; Liang *et al.*, 1998; Trainer *et al.*, 1991]. Production of hydroxyalkyl nitrates is examined here in order to evaluate this assumption.

We compute the mean and variance of potential HNO<sub>3</sub> production rates in the regional boundary layer surrounding Harvard Forest, using distributions of precursor concentrations for each month defined by means and logarithmic standard deviations of midday data (Table 3). We use surface measurements during the middle of the day, when vertical mixing is most intense, as the most representative of concentrations throughout the mixed layer. We exclude the high and low extremes (data outside the 12.5 and 87.5 percentiles) that occur in conditions that may not be regionally representative. Temperatures in the mixed layer are adjusted from the surface observations by a 6 °C km<sup>-1</sup> lapse rate. Regionally representative mixed-layer depths are taken from Holzworth [1967] to account for seasonal variation in mixing heights. Concentrations and temperature-adjusted rate constants [DeMore *et al.*, 1997] are applied to equations for the rate-limiting reaction in each pathway to yield a set of rates for HNO<sub>3</sub> production.

The homogeneous production of HNO<sub>3</sub> on a 24-hour average basis is given by  $k_1 \times [\text{OH}]$ , where [OH] is the 24-hour average OH concentration from a three-dimensional chemical tracer model [Wang *et al.*, 1998] that includes detailed NO<sub>x</sub> and hydrocarbon chemistry. The predicted OH seasonal cycle has an amplitude consistent with seasonal variations in hydrocarbon concentrations at Harvard Forest [Goldstein *et al.*, 1995]. The resulting production rates depend on seasonal variation in ambient NO<sub>2</sub> and OH concentrations.

We assume that heterogeneous formation of HNO<sub>3</sub> is limited by reaction (2) forming NO<sub>3</sub>. For typical particle concentrations in the continental boundary layer and a sticking coefficient,  $\gamma = 0.1$  [DeMore *et al.*, 1997], the lifetime of N<sub>2</sub>O<sub>5</sub> is shorter than the duration of night. Dentener and Crutzen [1993] computed the annual zonal mean lifetime for N<sub>2</sub>O<sub>5</sub> as <1 hour in northern midlatitudes below 850 mbar, due primarily to SO<sub>4</sub><sup>2-</sup> aerosol from anthropogenic sources. The reaction probability for NO<sub>3</sub> with aerosol surfaces in the continental boundary layer is 2 orders of magnitude less than that of N<sub>2</sub>O<sub>5</sub> [Rudich *et al.*, 1996]. The rate for heterogeneous formation of HNO<sub>3</sub> from hydrolysis of N<sub>2</sub>O<sub>5</sub> is given by  $2 \times \int_0^t k_4 [\text{O}_3][\text{NO}_2] dt$ . Because NO is fully oxidized to NO<sub>2</sub> at night, we initialize nighttime mixed-layer NO<sub>2</sub> concentrations with midday NO<sub>x</sub> (NO + NO<sub>2</sub>) and allow NO<sub>2</sub> to decay exponentially over time (NO<sub>2</sub> = NO<sub>x</sub>(0) exp(-k<sub>2</sub>O<sub>3</sub>t)). Fresh emis-

**Table 2b.** Mean Annual Cycle for N Deposition at Harvard Forest Derived From Seasonal Factors

Season	Deviation from annual mean <sup>a</sup> , μmol m <sup>-2</sup> d <sup>-1</sup>
Spring	16
Summer	16
Fall	-8
Winter	-24

<sup>a</sup>The value for the fourth season is set by the requirement that the seasonal cycle sum to zero

**Table 3.** Input Parameters for Estimation of Reaction Rates and Characteristic Times of NO<sub>y</sub> Reaction and Deposition

Month	NO <sub>y</sub> Deposit, μmol m <sup>-2</sup> d <sup>-1</sup>	NO <sub>y</sub>		NO <sub>x</sub>		NO <sub>2</sub>		O <sub>3</sub>		OH <sup>b</sup> , 10 <sup>6</sup> molecules. cm <sup>-3</sup>	T, °C	Mixing Height <sup>c</sup> , m
		Geometric Mean, pptv	lsd <sup>a</sup>	Geometric Mean, ppvt	lsd <sup>a</sup>	Geometric Mean, ppvt	lsd <sup>a</sup>	Arithmetic Mean, ppbv	s.d., ppbv			
Jan.	94.8	5254	0.51	3279	0.55	2688	0.58	27	5.24	0.1	-5	730
Feb.	91.3	6158	0.4	2796	0.56	2162	0.59	34	4.35	0.19	-4.4	900
March	121.9	5095	0.38	2110	0.5	1657	0.53	41	4.27	0.43	0.9	1200
April	139.4	3898	0.38	1282	0.54	1023	0.57	45	4.31	0.78	5.8	1800
May	159.4	3402	0.33	903	0.39	740	0.41	45	5.28	1.25	11.8	1800
June	128.2	2918	0.32	703	0.22	604	0.23	46	5.82	1.7	17.3	1800
July	183.7	3073	0.35	677	0.24	558	0.27	46	7.86	1.83	19.8	1800
Aug.	169.6	3547	0.33	772	0.34	661	0.35	44	6.18	1.5	19.2	1800
Sept.	131.9	3513	0.39	1138	0.44	920	0.47	35	4.75	0.89	14.3	1600
Oct.	122	5075	0.43	1979	0.52	1666	0.53	32	3.83	0.42	10.2	1500
Nov.	108.8	6737	0.43	3535	0.48	2974	0.5	27	3.44	0.16	3	1000
Dec.	107.8	5658	0.52	3226	0.49	2739	0.5	26	4.04	0.08	-2.1	750

Means and standard deviations for the concentrations are computed from the central 50% of the data for each month

<sup>a</sup> Standard deviation of log-transformed data.

<sup>b</sup> OH concentrations from Wang *et al.* [1998].

<sup>c</sup> Mixed-layer height from Holzworth, [1967].

sions only replenish NO<sub>x</sub> in the shallow nocturnal boundary layer. The rate expression is integrated over the length of night to obtain the production rate for HNO<sub>3</sub>. Concentrations of NO<sub>x</sub> and O<sub>3</sub> are negatively correlated, particularly in winter ( $r = -0.53$ ), but comparison of calculations using actual data and the random distributions for selected periods did not show any evidence of significant bias. The calculations presented here are intended to evaluate seasonal trends in the regional balance between deposition and HNO<sub>3</sub> production as defined by observed concentrations.

We compute rates for hydroxyalkyl nitrate formation based on the isoprene emissions at Harvard Forest (A. H. Goldstein *et al.*, Seasonal course of isoprene emissions from a midlatitude deciduous forest, submitted to *Journal of Geophysical Research*, 1997), a monoterpene:isoprene ratio of 0.25 [Guenther *et al.*, 1995], and hydroxyalkyl nitrate yields of 4.4% and 17% for isoprene and monoterpene, respectively. We make no distinction between direct dry deposition of the hydroxyalkyl nitrates, precipitation scavenging, conversion to HNO<sub>3</sub>, or condensation on aerosol surfaces; all processes result in transfer of reactive N from the atmosphere to the surface.

Computed rates for homogeneous production of HNO<sub>3</sub> at Harvard Forest show a seasonal cycle with a winter minimum, a flattened maximum from May through October, and a slight dip in July (Figure 10). The seasonal cycle is driven by seasonality in OH concentrations, but its amplitude is diminished by the offsetting effect of a winter maximum and summer minimum in NO<sub>2</sub> (M96). Rates for heterogeneous processes achieve their maxima in the spring and fall at the crossover points for opposing trends in NO<sub>x</sub> and O<sub>3</sub> concentrations (Figure 10, middle). Concentrations of NO<sub>x</sub> are at their peak in winter (M96), but lower O<sub>3</sub> concentrations and colder temperatures reduce rates for formation of NO<sub>3</sub>. Note that the variability for estimated heterogeneous HNO<sub>3</sub> production is greatest in the spring and fall months as well. Rapid NO<sub>x</sub> oxidation should occur during pollution episodes with elevated NO<sub>x</sub> and O<sub>3</sub>, with much slower rates at other times. Production of hydroxyalkyl nitrates begins in June and

reaches a maximum in July and August that is comparable to the inorganic HNO<sub>3</sub> production terms (Figure 10, bottom panel).

Computed rates for heterogeneous and homogeneous HNO<sub>3</sub> production roughly balance the mean deposition rate observed at Harvard Forest during winter and fall (Figure 11). In summer, however, inorganic production of HNO<sub>3</sub> does not balance the observed deposition. Concentration profiles at Harvard Forest are not consistent with NO<sub>2</sub> having a large deposition velocity (M96), but even a deposition velocity of 1 cm s<sup>-1</sup> would not account for the imbalance because NO<sub>2</sub> concentrations are too small. The apparent deficit in NO<sub>x</sub> oxidation during the growing season points to a mechanism linked to vegetation. The seasonality of hydroxyalkyl nitrate formation roughly matches the apparent excess in N deposition. However, its absolute magnitude is less certain, because mean hydrocarbon fluxes for the region must be estimated, and the complete chemical mechanism for this series of reactions has not been determined. Terpene emissions may be relatively more important in the spring and fall when conifers are active but oaks are dormant. The magnitude of hydroxyalkyl nitrate-mediated NO<sub>x</sub> oxidation that we estimate for the northeastern United States is in agreement with model predictions that this process accounts for 25% of the NO<sub>y</sub> deposition in North America during summer [Liang *et al.*, 1997].

At the remote site, near Schefferville, computed local production of HNO<sub>3</sub> is 2.2 μmol m<sup>-2</sup> d<sup>-1</sup> in summer, only about 10% of the observed average deposition, 20 μmol m<sup>-2</sup> d<sup>-1</sup>, but comparable to the minimum observed deposition (Figure 8). We noted previously that a few episodes accounted for a large proportion of the total N deposition at Schefferville, such as the rain event on July 30 and the elevated dry deposition on July 1-5 (Figure 8). Bakwin *et al.* [1994] attributed these events to advection of pollutants associated with passage of high-pressure systems that import depositing species of NO<sub>y</sub> from urban-industrial centers.

**4.3.2. Characteristic times for NO<sub>x</sub> oxidation and deposition.** We can directly estimate the time constants,  $\tau$ , for NO<sub>x</sub> oxidation by setting the concentrations of O<sub>3</sub> and OH to

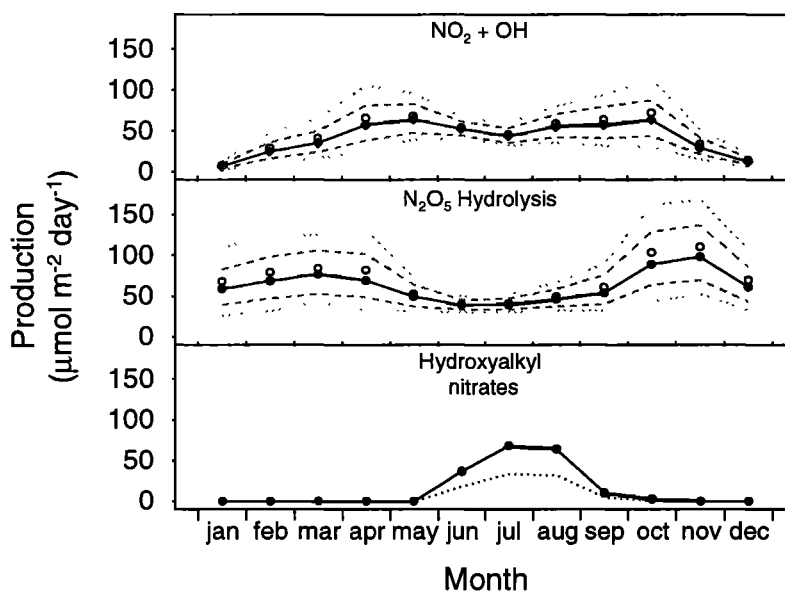


**Figure 10.** Computed production of HNO<sub>3</sub> by (top) NO<sub>2</sub> + OH and (middle) NO<sub>2</sub> + O<sub>3</sub> reactions for observed concentrations of NO<sub>x</sub>, NO<sub>2</sub>, O<sub>3</sub>, and air temperatures at Harvard Forest and typical values of OH and mixed layer depths in the northeastern United States. For each month, 1000 individual estimates of HNO<sub>3</sub> production were generated by using random values of concentrations picked from data distributions as defined in Table 3. The solid lines with solid circles indicate medians; open circles are the mean values. Long-dashed lines bound the twenty-fifth and seventy-fifth percentiles of the computed values; short-dashed lines are the standard deviations. (bottom) Potential production of hydroxyalkyl nitrates for the observed isoprene emission flux at Harvard Forest (solid line) and the production rate if the isoprene fluxes were a factor of 2 less (dashed line). Corresponding production rates at Schefferville are 1.6 and 0.6 μmol m<sup>-2</sup> d<sup>-1</sup> for homogeneous and heterogeneous pathways, respectively.

their monthly mean values (Table 3) and evaluating the relevant rate expression, for example,  $\tau = (k_1[\text{OH}])^{-1}$  for reaction (1). The characteristic time for deposition of NO<sub>x</sub> oxidation products is calculated as column mass divided by total

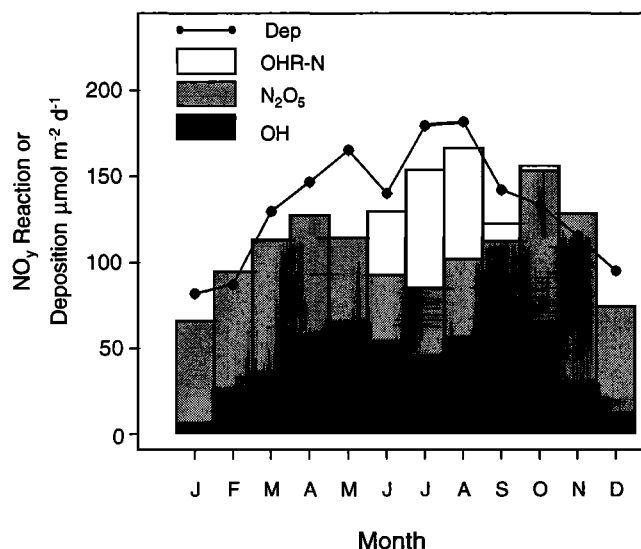


**Figure 11.** Total production of HNO<sub>3</sub> by homogeneous (dark shading), heterogeneous (light shading), and hydroxyalkyl nitrate (stippled) pathways in the mixed layer as estimated in Figure 10 versus observed N deposition (solid line) at Harvard Forest. Uncertainty estimates for the production and deposition terms (Figures 7 and 10) are omitted for clarity.

(wet plus dry) flux, analogous to the wet-deposition lifetimes reported by *Doddridge et al.* [1992] for NO<sub>y</sub> over Virginia. We estimated column mass by integrating the midday surface mixing ratio over the boundary layer depth ( $\int_0^X \rho(z) dz$ , where  $X$  is the mixing ratio and  $\rho$  is the air density). The characteristic time for hydroxyalkyl nitrate formation is determined from the NO<sub>x</sub> column mass divided by the scaled isoprene flux.

The characteristic times for both NO<sub>2</sub> oxidation by OH and hydroxyalkyl nitrate formation are <0.5 day in summer and increase at least ten fold in winter (Figure 12, top). However, the characteristic time for heterogeneous reaction is more uniform; thus the overall chemical lifetime increases from a minimum of 0.3 day in summer to only 1.5 days in winter as the limiting oxidant shifts from OH to O<sub>3</sub> (Figure 12). The characteristic time for removal of NO<sub>x</sub> oxidation products (NO<sub>y</sub>-NO<sub>x</sub>),  $\tau_{\text{dep}}$ , is around 1 day for most of the year and decreases to 0.4 day in winter when NO<sub>x</sub>:NO<sub>y</sub> is highest (Figure 12). The characteristic time expressed in terms of total NO<sub>y</sub>, which is the effective time constant for oxidation and deposition acting in series [*Parrish et al.*, 1991], ranges from 1 day in mid summer to more than 2 days in winter months. The shorter characteristic time for deposition of oxidation products in winter is consistent with shallower mixed layer and also with reduced contribution from non-depositing species, such as alkyl nitrates, to the mix of NO<sub>x</sub> oxidation products. These values are in agreement with the lifetimes that *Parrish et al.* [1991] find consistent with observed NO<sub>y</sub>:CO ratios in summer at Niwot Ridge.

At Schefferville, lower OH and O<sub>3</sub> concentrations account for chemical lifetimes of 1.0 day and 2.1 days, respectively,

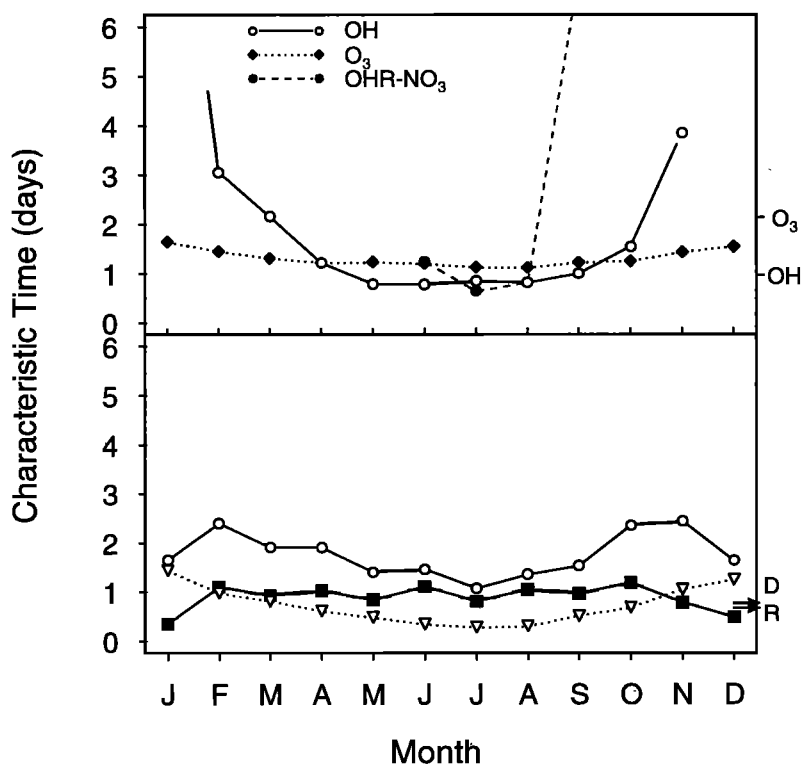


**Figure 12.** (top) Characteristic ( $e$ -folding) times for HNO<sub>3</sub> production estimated from modeled OH concentrations, monthly mean observed O<sub>3</sub> concentrations, and isoprene fluxes. (bottom) Deposition lifetimes for NO<sub>x</sub> (open circles) and for NO<sub>x</sub> oxidation products, NO<sub>y</sub> = NO<sub>y</sub> - NO<sub>x</sub>, (solid squares) are determined from the observed deposition flux and column mass. The overall chemical lifetime is the combination of characteristic times for reaction with OH, O<sub>3</sub>, and isoprene (dashed line with open triangles). The characteristic times for OH and O<sub>3</sub> oxidation (top) and the overall chemistry and deposition lifetimes (bottom) at Schefferville in summer are indicated by symbols on the right margin (OH, O<sub>3</sub>, R, D).

for oxidation by OH and O<sub>3</sub>. The characteristic time for deposition of NO<sub>y</sub> - NO<sub>x</sub> at Schefferville, 0.76 day, is slightly less than that at Harvard Forest.

Figure 12 shows that removal of NO<sub>x</sub> oxidation products (NO<sub>y</sub> - NO<sub>x</sub>) takes slightly longer than their production for most of the year. Hence, within the region surrounding Harvard Forest, NO<sub>x</sub> oxidation products tend to build up in relation to the total reactive N concentration. Relatively long lifetimes for deposition are consistent with the observation that some HNO<sub>3</sub> remains when an air parcel reaches a remote area such as Schefferville, where local oxidation of ambient NO<sub>x</sub> accounts for only 10% of NO<sub>y</sub> deposition. Because NO<sub>x</sub> oxidation is so rapid, the NO<sub>x</sub> observed at Schefferville is likely to arise from decomposition of PAN or other long-lived species transported there, rather than as NO<sub>x</sub> [Fan *et al.*, 1994]. Thus the fraction of NO<sub>x</sub> converted to stable organics is critical for supplying reactive N to the remote troposphere. Our results imply that, at Schefferville, NO<sub>x</sub> is provided by decomposition of reservoir species such as PAN [Singh and Hanst, 1981] and that PAN also supports background levels of NO<sub>y</sub>. Episodic transport of HNO<sub>3</sub> and other nonradical species accounts for high levels of NO<sub>y</sub> and pulses of N deposition.

Fluxes of NO<sub>x</sub> are a factor of 6 smaller ( $\approx e^{-2}$ ) at Schefferville than at Harvard Forest, somewhat less than the decline in concentration. Assuming comparable emission rates in source areas upwind, this finding suggests 2-3 days transport time to Schefferville.

**4.3.3. NO<sub>y</sub> budget integration.** From the differential equations for rates of NO<sub>x</sub> oxidation and deposition ( $d\text{NO}_x = -k_c\text{NO}_x dt$ , and  $d\text{HNO}_3 = (k_c\text{NO}_x - k_d\text{HNO}_3)dt$ , respectively) we can derive a simple expression to predict the concentration of HNO<sub>3</sub> in the boundary layer downwind of a major source region,

$$\text{HNO}_3(t) = \frac{\text{NO}_x(0)}{D} \left( \frac{k_c}{(k_d - k_c)} \right) (e^{-k_c t} - e^{-k_d t}). \quad (6)$$

Here HNO<sub>3</sub>( $t$ ) is the concentration of HNO<sub>3</sub> (and other rapidly deposited compounds) at time after emission,  $t$ , NO<sub>x</sub>(0) is the initial concentration of NO<sub>x</sub> at the emission source, and  $k_c$  and  $k_d$  are effective first-order rate constants (derived from photochemical calculations and from observations) for photochemical production and deposition, respectively. Note that  $k_c$  reflects heterogeneous, homogeneous, and organic pathways for conversion of NO<sub>x</sub> to HNO<sub>3</sub> (or other rapidly depositing species) and  $k_d$  accounts for total (wet plus dry) deposition. We include a dilution factor,  $D$ , to account for mixing of the polluted air parcel with cleaner background air ( $D$  cancels out of the analysis of ratios of species).

This ultra-simple model allows us to assess the fraction of NO<sub>x</sub> deposited in the region and the extent of the receptor area, using fluxes and concentrations of NO<sub>y</sub> observed at a single station. The model illustrates the consequences of seasonal trends in reaction and deposition rates and provides a first estimate for the fraction exported. We use mean concentrations and rates for chemical reactions and deposition, and

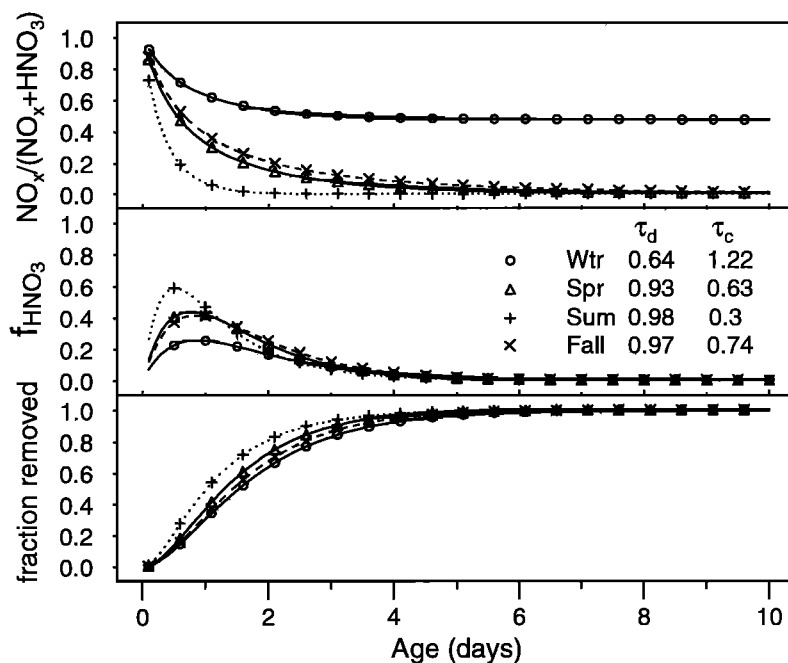


**Figure 13.** (top) Values of the NO<sub>x</sub> ratio, NO<sub>x</sub>/(NO<sub>x</sub>+HNO<sub>3</sub>), (middle) HNO<sub>3</sub> fraction,  $f_{\text{HNO}_3} = \text{HNO}_3(t)/(\text{NO}_x(0)/D)$ , and (bottom) fraction of NO<sub>x</sub> that has been deposited, computed from equation (6) (see text) by using seasonal mean values of reaction and deposition time constants (in days) for chemical reaction ( $\tau_r$ ) and deposition ( $\tau_d$ ) taken from Figure 12.

we treat individual parcels independently. In reality, oxidant concentrations, and hence reaction rates, depend somewhat on concentrations of NO<sub>x</sub> [Logan *et al.*, 1981], but the largest variations in the rates for deposition reflect seasonal changes in solar radiation, concentrations of water vapor, and boundary layer characteristics.

The model does not account for formation and recycling of PAN, which may have a long lifetime if it is transported above the boundary layer. The data analysis given above showed that the average reactive-N deposition rate at Harvard Forest closely matches the regional emission rate. Hence it is unlikely that the regional budget is strongly affected by ventilation of PAN from the boundary layer. However, the role of such processes in the supply of NO<sub>x</sub> to the global environment is unclear: the fraction escaping is predicted to be small [Horowitz *et al.*, 1998; Liang *et al.*, 1998] and consequently difficult to determine accurately by measurements of deposition.

The key feature of the boundary layer in summer, fall, and spring is that the NO<sub>x</sub> oxidation rate constant exceeds the deposition rate constant for the oxidation products; hence oxidation products make an increasing fraction of total NO<sub>y</sub>, and the ratio NO<sub>x</sub>/(NO<sub>x</sub>+HNO<sub>3</sub>) decreases with time (Figure 13, top). Observed values of NO<sub>x</sub>:NO<sub>y</sub> = 0.25 (M96) at noon during summer at Harvard Forest are consistent with transit times of <1 day, or mixtures of older emissions that have been depleted of NO<sub>x</sub> with fresh NO<sub>x</sub> emitted from sources a few hours upwind. Recycling of PAN may provide an input of NO<sub>x</sub> to maintain the NO<sub>x</sub>:NO<sub>y</sub> ratio at Schefferville near 0.2 (M96) rather than approaching 0 as predicted for transit times of >1 day. During winter the rate constant for deposition of NO<sub>x</sub> oxidation products exceeds the rate constant for NO<sub>x</sub> oxidation; the NO<sub>x</sub>/(NO<sub>x</sub>+HNO<sub>3</sub>) ratio for long times approaches a constant, ≈0.6, comparable to observed NO<sub>x</sub>:NO<sub>y</sub> ratios (M96).

The product of  $k_d \times f_{\text{HNO}_3}$  defines the fraction of initial NO<sub>x</sub> deposited in unit time at travel time  $t$  downwind, where  $f_{\text{HNO}_3}$  is the fraction of odd nitrogen present as HNO<sub>3</sub> relative to the initial NO<sub>x</sub> ( $f_{\text{HNO}_3} \equiv \text{HNO}_3(t)/\{\text{NO}_x(0)/D\} = k_c / (k_d - k_c) (e^{-k_c t} - e^{-k_d t})$ ). The value of  $f_{\text{HNO}_3}$  is zero at the emission source ( $t=0$ ), increases downwind to a maximum, and then gradually declines to 0 as NO<sub>x</sub> is oxidized and deposited (Figure 13, middle). Note that because the parcel is dispersing with time, concentrations and deposition per unit area typically decline with increasing distance from the source. For summer conditions the peak in  $f_{\text{HNO}_3}$  occurs at ages of <1 day, while for winter conditions with slower chemistry the peak is delayed and broadened such that  $f_{\text{HNO}_3}$  in winter exceeds the summer values for parcel ages of >2 days.

Integration of  $k_d \times f_{\text{HNO}_3}$  over time gives the cumulative fraction of NO<sub>x</sub> deposited (Figure 13, bottom): 45% for  $t = 1$  day in summer, 27% in winter. The time required to remove 95% of NO<sub>x</sub> is 3.5 days in summer and 5 days in winter. This analysis indicates that transport and dispersion of NO<sub>x</sub> in the boundary layer cannot account for most of the atmospheric N in the remote troposphere, because oxidation of NO<sub>x</sub> and deposition of HNO<sub>3</sub> are efficient. Observations of NO<sub>y</sub> accumulation in the wintertime troposphere at high latitudes [e.g. Bottenheim *et al.*, 1993; Dickerson *et al.*, 1985; Muthuramu *et al.*, 1994] could be accounted for by formation of stable species such as alkyl nitrates and PANs that have longer lifetimes but are not included in our analysis.

## 5. Conclusions

In this paper we have used 7 years of measurements at Harvard Forest, 1-2 days downwind of a major source region, to compute the rates for NO<sub>x</sub> oxidation and HNO<sub>3</sub> deposition, to determine the reactive-N budget at the site, and to estimate the fraction of N removed in the region near the source. We

found annual average input of 47 mmol m<sup>-2</sup> yr<sup>-1</sup>, with about twice as much wet as dry deposition. Variations in partitioning between wet and dry deposition tended to offset each other because HNO<sub>3</sub>, the main depositing species, is removed efficiently by both processes. Nitrogen deposition at Scheferville was a factor of ~6 less (20 μmol m<sup>-2</sup> d<sup>-1</sup> versus 130 μmol m<sup>-2</sup> d<sup>-1</sup>) during the summer than the mean summertime rate at Harvard Forest, consistent with a transport time of 2-3 days from emission sources.

Analysis of the regional balance between production and deposition allows us to infer reaction and deposition lifetimes for NO<sub>x</sub> in the boundary layer. The lifetimes for oxidation of NO<sub>x</sub> ranged from 0.24 day in summer, due to the combined effect of homogeneous, heterogeneous, and organic pathways, to 1.4 days in winter, due to heterogeneous processes alone. The lifetimes for deposition of HNO<sub>3</sub> were 1 and 0.6 day in summer and winter, respectively.

Our analysis shows that deposition of reactive N is regulated by the rate of oxidation of NO<sub>x</sub> by reactions with HO<sub>x</sub> radicals, by heterogeneous reactions of N<sub>2</sub>O<sub>5</sub>, and by organic pathways. Contributions from these three processes are comparable during summer; heterogeneous and organic pathways for NO<sub>x</sub> oxidation are more important than we expected them to be. The presence of forests downwind of source regions enhances rates for nitrogen deposition and increases the fraction of NO<sub>x</sub> retained in the region, because forests are efficient, aerodynamically rough receptors and because biogenic hydrocarbons emitted by vegetation accelerate the rate of oxidation of NO<sub>x</sub>.

The NO<sub>x</sub> emitted from eastern North America is efficiently retained in the region during summer. Export about doubles from summer to winter, but heterogeneous production of HNO<sub>3</sub> is efficient, and ventilation of the boundary layer is relatively slow; hence most of the emitted NO<sub>x</sub> is probably deposited further downwind. Thus remote sites such as Scheferville, 2-3 days' transport from the emission sources, could receive most of their annual reactive-N input during winter when it accumulates in the snowpack and becomes available during spring melt. Only a small fraction of N escapes to the global environment in either season.

**Acknowledgments.** This work was supported by grants from the National Aeronautics and Space Administration (NAG1-55, NAGW-3082), from the National Science Foundation (BSR-89-19300), from the U.S. Department of Energy to Harvard University (Northeast Regional Center of the National Institute for Global Environmental Change, DOE Cooperative Agreement DE-FC03-90ER61010), by Harvard University (Harvard Forest and Division of Applied Sciences), by the Electric Power Research Institute, and by the Alexander Host Foundation (fellowship to PSB). The Harvard Forest tower is a component of the Long-Term Ecological Research (LTER) site at Harvard Forest. We thank the staffs of the McGill Subarctic Research Station and the NASA Langley Research Center for logistical support at Scheferville during the ABLE 3B study. We thank the Harvard Forest woods crew for their assistance. We particularly thank B. Daube, A. Hirsch, S. Roy, D. Sutton, F. Gimmelfarb, and C. Nielsen for their contributions to this project. We thank D. Jacob, L. Horowitz, and Y. Wang for helpful discussions. The complete Harvard Forest data set is available from <http://www-as.harvard.edu>.

## References

- Aber, J. D., A. Magill, R. Boone, J. M. Melillo, P. Steudler, and R. Bowden, Plant and soil responses to chronic nitrogen additions at the Harvard Forest, Massachusetts, *Ecol. Appl.*, **3**, 156-166, 1993.
- Bakwin, P. S., et al., Reactive nitrogen oxides and ozone above a taiga woodland, *J. Geophys. Res.*, **99**, 1927-1936, 1994.
- Bottenheim, J.W., L. A. Barrie, and E. Atlas, The partitioning of nitrogen oxides in the lower Arctic troposphere during spring 1988, *J. Atmos. Chem.*, **17**, 15, 1993.
- Chambers, J. M., and T. J. Hastie (Eds.), *Statistical Models in S*, 608, pp. Wadsworth, Belmont, Calif., 1992.
- Davidson, E. A., Fluxes of nitrous oxide and nitric oxide from terrestrial ecosystems, in *Microbial Production and Consumption of Greenhouse Gases: Methane, Nitrogen Oxides, and Halomethanes*, edited by W. B. Whitman, pp. 219-235, Am. Soc. for Microbiol., Washington, D. C., 1991.
- DeMore, W. B., S. P. Sander, D. M. Golden, R. F. Hampson, M. J. Kurylo, C. J. Howard, A. R. Ravishankara, C. E. Kolb, and M. J. Molina, Chemical kinetics and photochemical data for use in stratospheric modeling, evaluation number 12, *JPL Pub.*, 97-4, 1997.
- Dentener, F. J., and P. J. Crutzen, Reaction of N<sub>2</sub>O<sub>5</sub> on tropospheric aerosols: Impact on the global distributions of NO<sub>x</sub>, O<sub>3</sub>, and OH, *J. Geophys. Res.*, **98**, 7149-7163, 1993.
- Dickerson, R. R., Reactive nitrogen compounds in the arctic, *J. Geophys. Res.*, **90**, 10,739-10,743, 1985.
- Doddridge, B.G., R. R. Dickerson, R. G. Wardell, K. L. Civerolo, and L. J. Nunnermacker, Trace gas concentrations and meteorology in rural Virginia, 2. Reactive nitrogen compounds, *J. Geophys. Res.* **97**, 20,631-20,646, 1992.
- Environmental Protection Agency (EPA), The 1985 NAPAP emission inventory (version 2): Development of the annual data and modeler's tapes, *Rep. EPA-600/7-89-012a*, Research Triangle Park, N. C., 1989.
- Fan, S.-M., D. J. Jacob, D. L. Mauzerall, J. D. Bradshaw, S. T. Sandholm, D. R. Blake, H. B. Singh, R. W. Talbot, G. L. Gregory, and G. W. Sachse, Origin of tropospheric NO<sub>x</sub> over subarctic eastern Canada in summer, *J. Geophys. Res.*, **99**, 16,867-16,877, 1994.
- Fitzjarrald, D. R., and K. E. Moore, Growing season boundary layer climate and surface exchanges in the northern lichen woodland, *J. Geophys. Res.*, **99**, 1899-1917, 1994.
- Galloway, J. N., W. H. Schlesinger, H. Levy II, A. Michaels, and J. N. Schoor, Nitrogen fixation: Anthropogenic enhancement-environmental response, *Global Biogeochem. Cycles*, **9**, 235-252, 1995.
- Goldstein, A. H., C. M. Spivakovsky, and S. C. Wofsy, Seasonal variations of nonmethane hydrocarbons in rural New England: Constraints on OH concentrations in northern midlatitudes, *J. Geophys. Res.*, **100**, 21,023-21,033, 1995.
- Goulden, M. L., J.W. Munger, S.-M. Fan, B. C. Daube, and S. C. Wofsy, Measurements of carbon sequestration by long-term eddy covariance: Methods and a critical evaluation of accuracy, *Global Change Biol.*, **2**, 169-182, 1996a.
- Goulden, M. L., J.W. Munger, S.-M. Fan, B. C. Daube, and S. C. Wofsy, Exchange of carbon dioxide by a deciduous forest: Response to interannual climate variability, *Science*, **271**, 1576-1578, 1996b.
- Guenther, A., et al., A global model of natural volatile organic carbon emissions, *J. Geophys. Res.*, **100**, 8873-8892, 1995.
- Hanson, P. J., and S. E. Lindberg, Dry deposition of reactive nitrogen compounds: A review of leaf, canopy and non-foliar measurements, *Atmos. Environ., Part A*, **25**, 1615-1634, 1991.
- Hoffmann, T., J. R. Odum, E. W. Bowman, D. H. Collins, D. Klockow, R. C. Flagan, and J. R. Seinfeld, Formation of organic aerosols from the oxidation of biogenic hydrocarbons, *J. Atmos. Chem.*, **26**, 189-222, 1997.
- Holland, E. A., et al., Variations in the predicted spatial distribution of atmospheric nitrogen deposition and their impact on carbon uptake by terrestrial ecosystems, *J. Geophys. Res.*, **102**, 15,849-15,866, 1997.
- Holzworth, G. C., Mixing depths, wind speeds and air pollution potential for selected locations in the United States, *J. Appl. Meteorol.*, **6**, 1039-1044, 1967.
- Horowitz, L.W., D. J. Jacob, J. L. Liang, and G. M. Gardner, Export of reactive nitrogen from North America during summertime: Sensitivity to hydrocarbon chemistry, *J. Geophys. Res.*, in press, 1998.
- Johnson, D. W. and S. E. Lindberg, *Atmospheric Deposition and Forest Nutrient Cycling*, 707 pp., Springer-Verlag, New York, 1992.
- Kames, J., and U. Schurath, Alkyl nitrates and bifunctional nitrates of atmospheric interest: Henry's law constants and their temperature dependencies, *J. Atmos. Chem.*, **15**, 79-95, 1992.

- Lefer, B. L., The chemistry and dry deposition of atmospheric nitrogen at a rural site in the northeastern United States, Ph.D. thesis, 119 pp., University of New Hampshire, December, 1997.
- Liang, J., D. J. Jacob, L. W. Horowitz, G. J. Gardner, and J. W. Munger, Seasonal budgets of reactive nitrogen species and ozone over the United States, and export fluxes to the global atmosphere, *J. Geophys. Res.* in press, 1998.
- Liu, S. C., M. Trainer, F. C. Fehsenfeld, D. D. Parrish, E. J. Williams, D. W. Fahey, G. Hubler, and P. C. Murphy, Ozone production in the rural troposphere and the implications for regional and global ozone distributions, *J. Geophys. Res.* 92, 4191-4207, 1987.
- Logan, J. A., M. J. Prather, S. C. Wofsy, and M. B. McElroy, Tropospheric chemistry: A global perspective, *J. Geophys. Res.*, 86, 7210-7254, 1981.
- Logan, J. A., Nitrogen oxides in the troposphere: Global and regional budgets, *J. Geophys. Res.*, 88, 10,785-10,807, 1983.
- Meyers, T. P., B. B. Hicks, R. P. Hosker Jr., J. D. Womack, and L. C. Satterfield, Dry deposition inferential measurement techniques, II, Seasonal and annual deposition rates of sulfur and nitrate, *Atmos. Environ., Part A*, 25, 2361-2370, 1991.
- Moody, J. L., J. W. Munger, A. H. Goldstein, D. J. Jacob, S. C. Wofsy, Harvard Forest regional-scale air mass composition by PATH (Patterns in atmospheric transport history), *J. Geophys. Res.*, in press, 1998.
- Munger, J. W., S. C. Wofsy, P. S. Bakwin, S.-M. Fan, M. L. Goulden, B. C. Daube, A. H. Goldstein, K. E. Moore, and D. R. Fitzjarrald, Atmospheric deposition of reactive nitrogen oxides and ozone in a temperate deciduous forest and a subarctic woodland, 1, Measurements and mechanisms, *J. Geophys. Res.*, 101, 12,639-12,657, 1996.
- Muthuramu, K., P. B. Shepson, J. W. Bottenheim, B. T. Jobson, H. Niki, and K. G. Anlauf, Relationships between organic nitrates and surface ozone destruction during Polar Sunrise Experiment 1992, *J. Geophys. Res.*, 99, 25,369-25,378, 1994.
- Nozière, B., I. Barnes, and K. Becker, Gas-phase oxidation of  $\alpha$ -pinene initiated by OH radicals in the presence of NO<sub>x</sub>: Product and mechanistic study; Identification and thermal stability of a terpenoid derived PAN analogue, paper presented at Workshop on biogenic hydrocarbons in the atmospheric boundary layer, Charlottesville, Aug. 24 to 27, 1997.
- Ollinger, S. V., J. D. Aber, G. M. Lovett, S. E. Millham, R. G. Lathrop, and J. M. Ellis, A spatial model of atmospheric deposition for the northeastern U. S., *Ecol. Appl.*, 3, 459-472, 1993.
- Parrish, D. D., M. Trainer, M. P. Buhr, B. A. Watkins, and F. C. Fehsenfeld, Carbon monoxide concentrations and their relation to concentrations of total reactive oxidized nitrogen at two rural U.S. sites, *J. Geophys. Res.*, 96, 9309-9320, 1991.
- Paulson, S. E., and J. H. Seinfeld, Development and evaluation of a photooxidation mechanism for isoprene, *J. Geophys. Res.*, 97, 20,703-20,715, 1992.
- Prather, M., R. Derwent, D. Ehhalt, P. Fraser, E. Sanhueza, and X. Zhou, Other trace gases and atmospheric chemistry, in *Climate Change 1994: Radiative Forcing of Climate Change and an Evaluation of the IPCCIS92 Emission Scenarios*, chap. 2, Cambridge Univ. Press, Cambridge, 1995.
- Roberts, J. M., The atmospheric chemistry of organic nitrates, *Atmos. Environ.* 24A, 243-287, 1990.
- Rudich, Y., R. K. Talukdar, A. R. Ravishankara, and R. W. Fox, Reactive uptake of NO<sub>3</sub> on pure water and ionic solutions, *J. Geophys. Res.*, 101, 21,023-21,231, 1996.
- Schindler, D. W., and S. E. Bayley, The biosphere as an increasing sink for atmospheric carbon: Estimates from increased nitrogen deposition, *Global Biogeochem. Cycles*, 7, 717-733, 1993.
- Shepson, P. B., E. Mackay, and K. Muthuramu, Henry's Law constants and removal processes for several atmospheric  $\beta$ -hydroxy alkyl nitrates, *Environ. Sci. Technol.*, 30, 3618-3623, 1996.
- Singh, H. B., and P. L. Hanst, Peroxyacetyl nitrate (PAN) in the unpolluted atmosphere: An important reservoir for nitrogen oxides, *Geophys. Res. Lett.*, 8, 941-944, 1981.
- Tjepkema, J. D., R. J. Cartica, and H. F. Hemond, Atmospheric concentration of ammonia in Massachusetts and deposition on vegetation, *Nature*, 294, 445-446, 1981.
- Trainer, M., et al., Observations and modeling of the reactive nitrogen photochemistry at a rural site, *J. Geophys. Res.*, 96, 3045-3063, 1991.
- Tuazon, E. C., and R. Atkinson, A product study of the gas-phase reaction of isoprene with the OH radical and the presence of NO<sub>x</sub>, *Int. J. Chem. Kinet.*, 22, 1221-1236, 1990.
- Wang, Y., J. A. Logan, and D. J. Jacob, Global simulation of tropospheric O<sub>3</sub>-NO<sub>x</sub>-hydrocarbon chemistry, 2., Model evaluation and global ozone budget, *J. Geophys. Res.*, in press, 1998.
- Wedin, D. A., and D. Tilman, Influence of nitrogen loading and species composition on the carbon balance of grasslands, *Science*, 274, 1720-1723, 1996.

P. S. Bakwin, Climate Monitoring and Diagnostics Laboratory, National Oceanic and Atmospheric Administration, 325 Broadway, Boulder, CO 80303.

A. S. Colman, Department of Geology and Geophysics, Yale University, New Haven, CT 06511.

S.-M. Fan, Atmospheric & Oceanic Sciences Program, Princeton University, Princeton, NJ 08544.

A. H. Goldstein, Department of Environmental Science, Policy, and Management, University of California, Berkeley, Berkeley, CA 94720.

M. L. Goulden, Department of Earth System Science, University of California, Irvine, Irvine, CA 92697-3100.

J. W. Munger and S. C. Wofsy, Department of Earth and Planetary Sciences, Harvard University, 20 Oxford Street, Cambridge, MA 02138. (e-mail: jwm@io.harvard.edu; scw@io.harvard.edu)

(Received April 22, 1997; revised January 5, 1998; accepted January 9, 1998.)